Calcium phosphate nucleation on surface-modified PTFE membranes

LISBETH GRØNDAHL†, FRANCISCO CARDONA, KHANG CHIEM, EDELINE WENTRUP-BYRNE*
Centre for Instrumental and Developmental Chemistry, Queensland University of Technology, GPO Box 2434, Brisbane QLD 4001, Australia
E-mail: e.wentrupbyrne@qut.edu.au

THOR BOSTROM
Analytical EM Facility, Queensland University of Technology, GPO Box 2434, Brisbane QLD 4001, Australia

Highly porous PTFE membranes are currently being used in facial reconstructive surgery. The present study aims at improving this biomaterial through creating a more bioactive surface by introducing ionic groups onto the surface. The unmodified PTFE membrane does not induce inorganic growth after immersion in simulated body fluid (SBF) for up to 4 weeks. Copolymeric grafting with acrylic acid (AAc) by means of gamma irradiation and subsequent *in vitro* testing in SBF reveals that this copolymer initially acts as an ion-exchange material and subsequently induces growth of a calcium phosphate phase (Ca/P = 2.7) when large amounts (15%) of pAAc are introduced onto the membrane surface. This copolymer is not expected to function well from a biomaterials perspective since SEM showed the pores on the surface to be partly blocked. In contrast, the surface of monoacryloxyethyl phosphate (MAEP)-modified samples is altered at a molecular level only. Yet the modified materials are able to induce calcium phosphate nucleation when the external surface coverage is 44% or above. The initial inorganic growth on these membranes in SBF has a (Ca + Mg)/P ratio of 1.1 (presumably Brushite or Monetite). The secondary growth, possibly calcium-deficient apatite or tricalcium phosphate, has a (Ca + Mg)/P ratio of 1.5. This result is a promising indicator of a bioactive biomaterial.

1. Introduction

The development of new and improved medically useful bone-substitute materials is severely limited due to an incomplete understanding of the specific surface requirements of a biomaterial intended for a particular use. Since the initial interaction of an implant with the body is through its surface, the initial acceptance of any foreign material is largely dependent on its surface properties [1, 2]. For many biomaterials a fibrous connective tissue layer that effectively separates the bone from the implant is formed. This results in poor osseointegration at the bone-implant interface and may result in loosening of the implant, destruction of the tissue near the implant site, pain, and subsequent expensive and intrusive revision surgery.

Introduction of functional groups on the surface of polymeric materials or incorporating functional groups within a polymeric framework are strategies, which have aimed at improving the biocompatibility of bone-substitute materials by providing a nucleation site for calcium hydroxyapatite ($Ca_{10}(PO_4)_6(OH)_2$, HAP). Grafting phosphate-containing monomers onto polyethylene materials resulted in doubling the amount of HAP growth on the modified material in simulated body fluid (SBF) whereas a smaller effect was observed for the acrylic acid (AAc)-grafted material [3]. Subsequent histologic studies on the phosphate-modified polyethylene material showed a significantly enhanced interface of the implant surface with the newly formed bone. This was attributed to the phosphate groups providing nucleation sites for HAP growth [4]. Another study which looked at the ability of HAP to form on copolymers containing phosphinyl groups showed a linear dependence on the phosphate content of each polymer [5]. Furthermore, a dependence on the structure of the polymer was observed; polymers with the phosphorus containing groups ''buried'' within the bulk polymer failed to induce HAP formation and thus, it was suggested that phosphorus-containing groups on the surface of the polymer acted as active centers for nucleation. In a recent study, the side chains of degradable tyrosine-derived polycarbonates were

* Author to whom all correspondence should be addressed.
† Present address: Department of Chemistry, University of Queensland, Brisbane QLD 4072, Australia.

changed to include high numbers of carboxylic acid groups yielding a biomaterial, which exhibited direct bone apposition greater than non-modified polycarbonates [6]. The resulting improvement was attributed to the ability of the carboxylate groups on the surface to chelate calcium ions and thereby create nucleation sites for HAP formation. In yet another study in which poly(ethylene glycol) was grafted onto the surface of bamboo a continuous layer of a calcium phosphate phase formed in SBF [7]. It was rationalized that calcium chelation by the grafted-polyether layer on the bamboo surface caused high local calcium concentrations thereby providing a nucleation site for the calcium phosphate phase.

Further evidence for the ability of functional groups to induce HAP growth comes from a study aimed at gaining a better understanding of the nature of the inorganic–organic interface interaction in the body environment. The study involved HAP formation on organic monolayers in a simulated-body environment and have shown that the growth rate is highly dependent on the end-group of the organic molecules [8]. A very high growth rate is observed for phosphate functionalized molecules whereas a slightly lower rate is observed for molecules with carboxylate end groups. Amides and amines on the other hand show very low growth rates. Clearly, negatively charged groups, and in particular phosphate, strongly induce apatite formation whereas positively charged groups do not.

The use of SBF to test the biocompatibility of materials *in vitro* was first developed by Kokubo *et al*. [9]. They found that when bioactive glass-ceramics were soaked in solutions with pH and ion concentrations of inorganic species almost equal to that of human blood plasma (Table I), a bone-like apatitic layer formed on the surface. Since such apatite formation is not observed on glass-ceramics considered bio-inactive, they concluded that apatite formation in SBF is an indication that the synthetic material is capable of bonding with living bone. A large variety of materials including surface-modified silk fabrics [10], surface-modified cotton [11, 12], titanium metal [13], silica gel [14, 15], and various polymers [3, 16, 17] have since been evaluated on the basis of their performance in SBF. Although there is evidence that a correlation between *in vitro* apatite formation and *in vivo* bone bonding exists for many materials, it is not always possible to reach unequivocal conclusions about bioactivity from SBF *in vitro* experiments [18]. Currently, however, it is the simplest non-cellular *in vitro* test available and will provide information on calcium phosphate growth in all cases. This is generally accepted as an important property for bone-substitute materials in order for them to bond to living bone [1].

In this study we investigated calcium phosphate nucleation in a simulated-body environment on porous poly(tetrafluoroethylene) (PTFE) which had been surface modified with either phosphate groups (by grafting monoacryloxyethyl phosphate, MAEP, Fig. 1) or carboxylate groups (by grafting AAc, Fig. 1). A more comprehensive understanding of the *in vitro* performance of a biomaterial is possible through a combination of studies with not only SBF but also with specific proteins and cells. We are currently undertaking such studies.

Highly porous expanded PTFE (ePTFE) is currently being used in facial reconstructive surgery. Studies have shown that ePTFE performs well in animals [19] as well as in humans [20]. However, depending on the specific purpose for which it is intended the implant material is not always an ideal bone substitute and we therefore chose this material to investigate the effect of introducing surface-active groups.

2. Materials and methods

2.1. Materials

Poly(tetrafluoroethylene) ''020-40'' membranes from Sumitomo (mean pore diameter 1.10 μm [21], membrane thickness 70 μm and crystallinity 18% [22]) were washed by soxelet extraction in methanol for 12 h and subsequently dried in a vacuum oven. AAC was from Aldrich. All reagents were of analytical grade and deionized water (MilliQ) was used throughout.

2.2. Graft Polymerization

The preparation of MAEP-grafted PTFE membranes has previously been described [22]. Graft polymerization of AAc onto PTFE was carried out using gamma irradiation with a Gamma-cell 220 using a Cobalt-60 source with a dose rate of approximately 7.6 kGy/h. The polymer membrane ($1 \times 1\,cm^2$) was placed in aqueous solutions (3 ml) containing concentrations of 1, 10 or 20% (w/w) AAc. Dissolved oxygen was removed by bubbling with nitrogen gas for 10 min. After being subjected to a dose of 10 kGy the membranes were washed with MilliQ water overnight at 60 °C to remove any loose homopolymer occluded onto the grafted membrane. The membranes were then dried under vacuum overnight.

2.3. Calcium phosphate growth in SBF

Calcium phosphate formation on the surface-modified as well as unmodified PTFE membranes was evaluated by immersing the membranes in SBF. This is a well-established method of determining surface susceptibility to apatite growth since SBF contains inorganic ions in concentrations similar to that of human blood plasma (Table I).

The SBF solution was prepared as described by Tas [23] by dissolving NaCl (99.9%), $NaHCO_3$ (99.0%), KCl

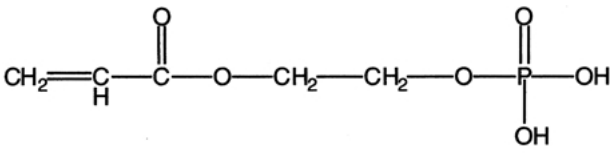

Monoacryloxyethyl Phosphate (MAEP)

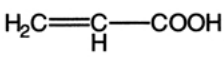

Acrylic Acid (AAc)

Figure 1 Chemical structures of AAc and MAEP monomers.

TABLE I Ion concentrations (mM) in SBF and human blood plasma

Ion	Na^+	K^+	Mg^{2+}	Ca^{2+}	Cl^-	HCO_3^-	HPO_4^{2-}	SO_4^{2-}
SBF	142.0	5.0	1.5	2.5	125.0	27.0	1.0	0.5
Plasma	142.0	5.0	1.5	2.5	103.0	27.0	1.0	0.5

(99.5%), Na_2HPO_4 (99.0%), $MgCl_2 \cdot 6H_2O$ (99.0%), $CaCl_2 \cdot 2H_2O$ (99.5%), Na_2SO_4 (99.0%) in pre-boiled water at room temperature. The solution was buffered to a pH of 7.4 with HCl and $(CH_2OH)_3CNH_2$ (99.8%) at 36.5 °C. Individual membrane pieces were placed in polystyrene containers, 25 ml SBF were added (membrane pieces floated and were held in the center of the container by means of inert plastic netting) and placed in a water bath maintained at 36.5 ± 0.2 °C. The SBF solution was renewed every 3 days for studies of 1 week duration and every 6 days for studies of 2 or 4 weeks duration. pH measurements on the exchanged solutions showed that the pH did not differ from the original solution of pH 7.4 ± 0.1. After a set time the membranes were removed from the solutions, washed thoroughly with water and dried at 80 °C overnight.

2.4. Characterization

The degree of grafting was determined from the increase in weight of the sample from the formula:

$$\text{Grafting yield}(\%) = 100 \times (w_g - w_i)/w_i$$

where w_g is the weight of grafted sample and w_i is the weight of initial sample.

X-ray photoelectron spectroscopy (XPS) was used to analyse the yields of external surface coverage. XPS survey (0.5 eV resolution) and multiplex (0.1 eV resolution) scans were recorded on a Perkin-Elmer PHI model 560 spectrometer with a double-pass cylindrical mirror analyser, and a vacuum system giving a base pressure of $\sim 10^{-9}$ Torr. X-rays were generated from a MgKα source (1253.6 eV). The binding energy of samples was calibrated using that of the F(1s) peak (689.7 eV) [24].

Fourier transform infra red (FTIR) transmittance spectra (520 scans, 4 cm^{-1} resolution, wave number range 400-4000 cm^{-1}) were recorded using a Nicolet Nexus FTIR Spectrometer with continuum microscope. An aperture area of $100 \times 100\,\mu m^2$ was used. FTIR micro-attenuated total reflectance (μ-ATR) spectra (128 scans, 4 cm^{-1} resolution, wave number range 400–4000 cm^{-1}) were collected using a μ-ATR detector equipped with a silicon crystal (refractive index of 3.49 (589 nm) and an average angle of incidence of 35°) using a Nicolet Nexus FTIR spectrometer. Spectra were measured from a $100 \times 100\,\mu m^2$ area. The depth penetration varied from 0.6 μm (at 500 cm^{-1}) to 5 μm (at 4000 cm^{-1}), for an estimated refractive index of the polymer/CaP phase of 1.5. All FTIR spectra were recorded at ambient temperature.

2.5. Electron microscopy and X-ray microanalysis

Scanning electron microscopy (SEM) of gold or carbon coated samples was performed using a JEOL 35CF scanning electron microscope, which was equipped with a Meeco ImageSlave digital image acquisition system. Energy-dispersive X-ray microanalysis (EDX) of inorganic material on the membrane surfaces was carried out on carbon coated samples using a JEOL 840A electron probe microanalyser equipped with a NORAN Be-window Si/Li X-ray detector and a Moran Scientific PC-based X-ray microanalysis system for quantitative bulk sample microanalysis. A calcium hydroxyapatite standard was used to standardize for Ca and P. Samples for transmission electron microscopy (TEM) were prepared by scraping off small pieces of the inorganic material from the surface of the PTFE membrane, suspending the material in ethanol, dispersing it onto copper TEM grids coated with a thin Formvar-carbon support film, and allowing the suspension to air dry. Elemental microanalysis of these samples was carried out on a Philips CM200 TEM equipped with a Link thin-window X-ray detector capable of detecting C and O, and a Link ISIS X-ray microanalysis system (Oxford Instruments, UK). Crystallinity of the material was checked by selected area electron diffraction.

3. Results and discussion

3.1. Grafting of AAc onto PTFE membrane

Three different reaction conditions were used for grafting AAc onto PTFE membranes. In all cases a gamma irradiation dose of 10 kGy was used together with different monomer concentrations (Table II). XPS survey scans of samples A1–A3 showed major peaks assigned to F, O and C and minor peaks assigned to N and

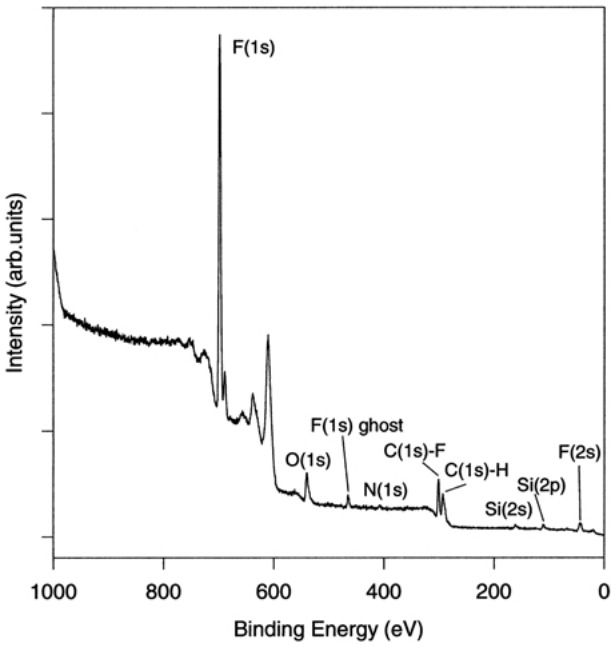

Figure 2 XPS survey scan of sample A3.

TABLE II Grafting yield and external surface coverage (atomic ratios determined from XPS multiplex scans) for AAc-grafted onto PTFE membranes

Sample	Monomer conc. (%)	Grafting yield (%)	CH/(CH + CF) atomic ratio
A1	1.0 (water)	< 0.5	0.44
A2	10.0 (water)	2.4	0.49
A3	20.0 (water)	14.9	0.43

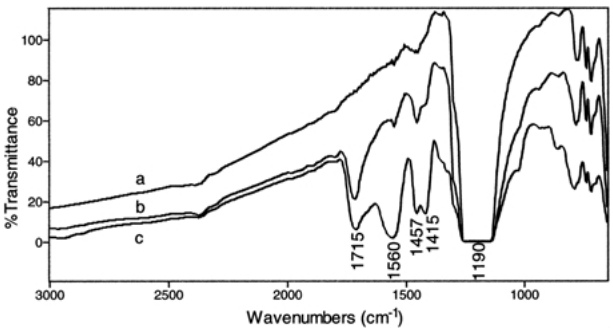

Figure 3 FTIR transmittance spectra of (a) unmodified PTFE membrane, (b) AAc-grafted membrane A2, and (c) AAc-grafted membrane A3.

Si which are due to an unknown impurity (Fig. 2). For all samples successful grafting was verified by XPS.

FTIR transmittance spectra of the non-grafted membranes show C–F stretching vibrations at 1150 and 1210 cm^{-1} [25]. For the grafted samples A1–A3 these vibrations are observed as a broad band at 1190 cm^{-1}. FTIR transmittance micro-spectroscopy of a $100 \times 100\ \mu m^2$ area providing evidence for the formation of AAc-grafted PTFE membrane (Fig. 3). Because the spectra are measured through the full 70 µm of the sample, the broad band in the 1190 cm^{-1} region is saturated. A small band at 1715 cm^{-1}, which can be assigned to the carbonyl stretch of the carboxylic acid, is observed in sample A1. This band increased in samples A2 and A3, indicating an increase in grafting yield. Additional bands are observed, one at 1457 cm^{-1} is assigned to methylene stretches, and two at 1560 and 1415 cm^{-1} (in sample A3) are assigned to the carbonyl stretch of the carboxylate ion. The presence of deprotonated carboxylic acid groups is attributed to water in the sample since no cations are observable in the XPS survey scans.

The grafting yield, as determined from the weight increase of the membrane, increased with increasing monomer concentration (Table II). Whereas in sample A1 only a small amount of AAc has been grafted onto the membrane, in samples A2 and A3 polymeric grafting of poly(acrylic acid) (pAAc) has occurred. In contrast, the external surface coverage, as determined from the atomic ratio obtained from XPS multiplex scans, was constant (within experimental error) for all three samples (Table II). The grafting yields obtained in this study are lower than previously reported [26, 27]. This is explained by the different reaction conditions of higher monomer concentration (30 or 40%), higher radiation doses (up to 100 kGy), and the use of an inhibitor ($FeCl_3$). However, since our aim was to produce PTFE membranes with only small amounts of grafted AAc in order to have a comparable coverage to the MAEP-grafted PTFE membranes this was not an issue [22].

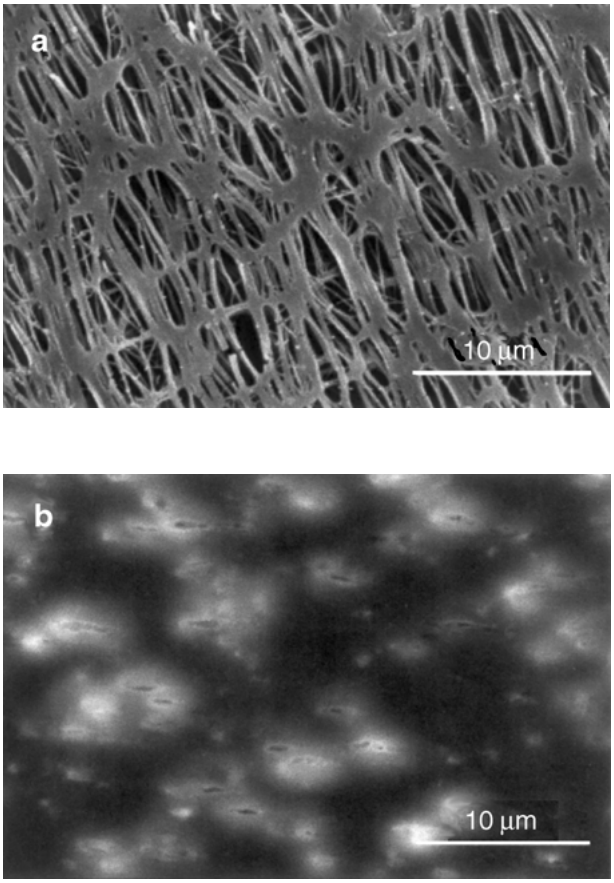

Figure 4 Scanning electron micrographs of (a) unmodified PTFE membrane and (b) AAc-grafted membrane sample A3.

As evident from SEM images (Fig. 4) the formation of pAAc in sample A3 actually changes the structure of the material. A pAAc layer covers a large portion of the membrane leaving only small gaps of less than 2 µm through which the original PTFE membrane can be seen. This is in contrast to the MAEP-modified PTFE samples, which show no visual difference from the unmodified membrane [22].

3.2. Immersion in SBF

In the present study, the ability of untreated PTFE membranes as well as AAc and MAEP-grafted membranes to induce calcium phosphate growth in SBF was investigated. Each membrane was immersed in 25 ml of SBF and placed in a thermostated water bath at 36.5 °C. The solutions were changed on a regular basis; the pH proved to be stable ($pH = 7.4 \pm 0.1$) over the growth period. After the membranes had been washed and dried in an oven at 80 °C overnight they were characterized using FTIR µ-ATR spectroscopy, and SEM coupled with EDX.

According to SEM, the unmodified PTFE membrane showed no calcium phosphate deposit after up to 4 weeks in SBF (i.e. it looked identical to that of Fig. 4(a)). This finding is very important since it means that any calcium phosphate growth on the surface-modified membranes can be attributed to the introduced functional groups.

3.3. AAc-modified PTFE membranes after immersion in SBF

As described above, the three AAc-grafted membranes all displayed the same degree of external surface coverage but differed with respect to the degree of grafting (Table II). Of these membranes only sample A3 had enough inorganic growth to be observable using light microscopy. The FTIR μ-ATR spectrum $100 \times 100\,\mu m^2$ of sample A3 after 2 weeks in SBF shows two notable features (Fig. 5(b)). First, compared to the spectrum of the sample A3 before immersion in SBF (Fig. 5(a)), the band corresponding to the carbonyl vibration of the carboxylic acid groups ($1715\,cm^{-1}$) has disappeared and the bands arising from the carbonyl vibration of the carboxylate groups (1560 and $1415\,cm^{-1}$) have increased. It is evident that AAc-grafted PTFE membrane A3 is in part behaving as an ion-exchange material in SBF by substituting all of the carboxylic acid protons with calcium ions. Second, a large broad band around $1045\,cm^{-1}$ is present in the spectrum of sample A3 after 2 weeks in SBF (Fig. 5(b)). This band is assigned to phosphate vibration modes [28] rather than sulfate or carbonate vibration modes, ions which are also present in SBF. However, carbonate does not display vibration modes in this region and sulfur is not detected in significant amounts by EDX. Clearly, this indicates that the inorganic material contains phosphate ions. A ratio of 1 : 1 of carboxylate to phosphate content is obtained from integration of their respective vibration bands. Thus, the inorganic phase formed on membrane A3 contains significant amounts of carboxylate groups.

An examination of the three AAc-grafted PTFE membranes after 2 weeks in SBF using SEM showed growth of a mineral phase only on sample A3 (Fig. 6(a)). No calcium phosphate growth was detected by SEM on samples A1 and A2. This is in agreement with the light microscopy results. EDX of the inorganic material on sample A3 revealed that although it contained principally calcium and phosphate with a Ca/P atomic ratio of 2.7, some sodium and magnesium (Ca + Na + Mg/P ratio of 3.1) were also present, Fig. 7(c). Membrane areas with no visible inorganic crystal growth (i.e. no discrete particles) showed Ca/P ratios of around 3. However, since the inorganic growth was very thin the ratios are associated with large errors.

The very high Ca/P ratio can in part be explained by the contribution from the carboxylate-bound calcium ions present. Another possible explanation proposed by Mucalo *et al*. [29] to explain their high Ca/P ratios of calcium phosphate coatings on Ca^{2+} saturated ion-exchange resins is a ''leaching'' of excess Ca^{2+} from the interior of the resin into the coating. It is, however, also possible that some $Ca(OH)_2$ and/or $CaCO_3$ is present. Bands in the infrared at $\sim 3600\,cm^{-1}$ are usually indicative of hydroxide species, and a strong band at $1490–1410\,cm^{-1}$ is indicative of $CaCO_3$ minerals. A close examination of the FTIR spectrum of sample A3 (Fig. 5(b)) failed to show these typical bands. However, since the $CaCO_3$ region overlaps with the pAAc vibrations in sample A3 (1457 and $1415\,cm^{-1}$) it is not possible to categorically exclude $CaCO_3$ although it is clear that it would only be present as a minor component.

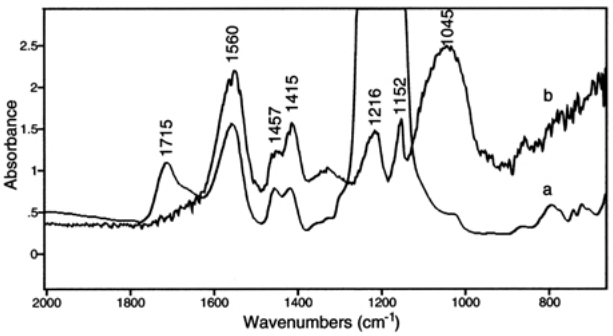

Figure 5 FTIR μ-ATR spectra of (a) AAc-grafted PTFE membrane A3, (b) inorganic material on AAc-grafted membrane A3.

3.4. SBF studies of MAEP-modified PTFE membranes

The ability of MAEP grafted PTFE membranes to induce calcium phosphate growth was examined for a range of membranes (Table III). The MAEP grafted samples have a variable amount of the monomer incorporated onto the PTFE membrane (up to 10%), and display a large range in external surface coverage (30–99%), Table III.

FTIR μ-ATR spectroscopy was used to analyze membrane P6 after 1 week in SBF. The spectrum of the grafted membrane (Fig. 8(a)) shows C–F stretching vibrations at 1152 and $1216\,cm^{-1}$ due to the PTFE membrane [25]. Carbonyl stretching vibrations at $1727\,cm^{-1}$ and methylene vibrations at $1435\,cm^{-1}$ indicate successful grafting [22, 30]. Light microscopy of the same membrane after 1 week in SBF shows that some areas are covered with an inorganic material whereas in other areas no deposits can be seen. A spectrum recorded from the surface of the inorganic growth (Fig. 8(b)) shows no signals from the PTFE membrane although vibration bands from the grafted monomer are visible. These bands are positioned at 1072, 997, and $955\,cm^{-1}$ and display different relative intensities compared to those of Fig. 8(a). Phosphate vibrations in the 500-$1200\,cm^{-1}$ region are usually used to establish which calcium phosphate mineral phase is present [28]. Unfortunately, in the MAEP-grafted samples the vibrations from the monomer overlap with

TABLE III Grafting yield (phosphate analysis [22]) and external surface coverage (atomic ratios determined from XPS multiplex scans) for MAEP-grafted onto PTFE membranes

Sample	Grafting yield (μg/mg)	CH/(CH + CF) atomic ratio
P1	—	0.30
P2	—	0.36
P3	14	0.44
P4	—	0.68
P5	80	0.85
P6	56	0.90
P7	50*	0.90
P8	25	0.93
P9	69	0.93
P10	70*	0.94
P11	98	0.99

—, not determined; *, from relative intensities of signals in the FTIR PAS spectrum [22].

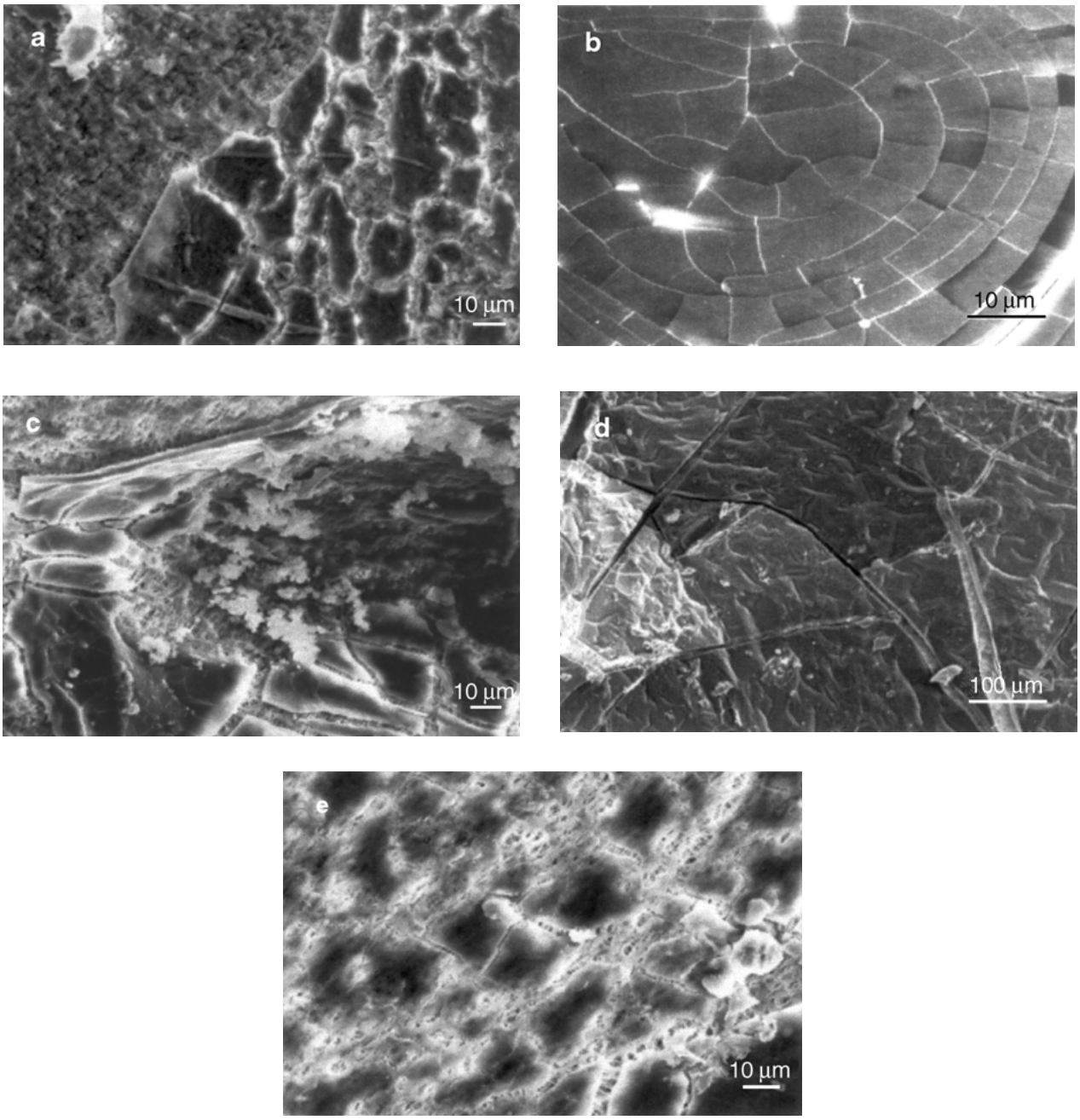

Figure 6 Scanning electron micrographs of (a) membrane A3 after 2 weeks in SBF, (b) membrane P4 after 1 week in SBF, (c) membrane P5 after 1 week in SBF, (d) membrane P8 after 1 week in SBF, (e) different area of membrane P8 after 1 week in SBF.

this region, and the minor shifts in band position and relative intensity do not provide conclusive information, thus making it difficult to interpret the spectra of the inorganic material. Scraped off inorganic material from sample P6 was examined by TEM and showed that the major component which contained the elements Ca, P, Mg, C, and O (Ca/P = 0.9–1.1, from EDX on TEM) appeared amorphous as seen from a lack of distinct rings or spots in the electron diffraction patterns. Furthermore, EDX in TEM identified minor components correlated with $CaCO_3$ and other compounds containing combinations of ions from the SBF solution.

The FTIR spectrum of sample P6 after 1 week in SBF of an area showing no inorganic growth (Fig. 8(c)) shows only vibrations from PTFE. Thus, there seems to be a direct correlation between the presence of grafted-MAEP chains and the growth of an inorganic phase. It has been found that the grafting of MAEP onto PTFE membranes occurs in a manner that has been described as patchy and uneven [22] and this could explain the uneven growth of inorganic material in SBF. Ratzsch *et al*. [31] have proposed ''grafting by nests'' as a possible explanation for such uneven grafting.

Examination of samples P1 and P2 using SEM showed that no significant calcium phosphate nucleation had occurred. Scarce, small particles of calcium and phosphate-rich inorganic materials could be found on these samples but these materials also contained high levels of silica indicating that nucleation of the calcium phosphate materials has probably taken place on silica contaminations on the membranes. The remaining MAEP-modified PTFE samples, which displayed external MAEP surface coverage ranging from 44% to 99% all induced calcium phosphate nucleation in varying degrees: sample P3 showed a scarce distribution of large inorganic deposits and the coverage of such deposits

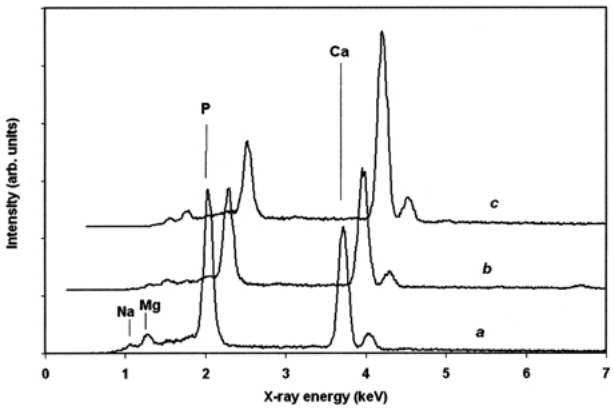

Figure 7 EDX spectra of (a) inorganic growth on sample P5 (Ca/P = 1.02), (b) secondary growth on sample P5 (Ca/P = 1.43), and (c) inorganic growth on sample A3 (Ca/P = 2.74).

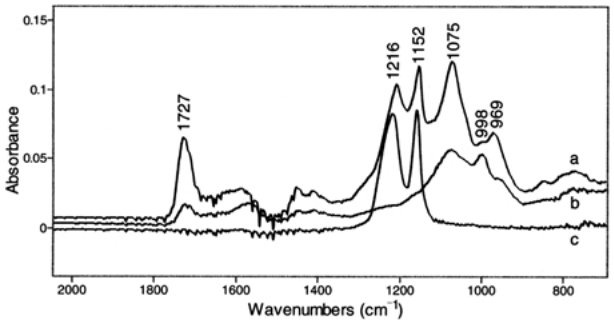

Figure 8 FTIR μ-ATR spectra of (a) MAEP-grafted PTFE membrane P6, (b) inorganic material on of MAEP-grafted membrane P6, (c) area between inorganic materials of MAEP-grafted membrane P6.

increased with increasing external surface grafting yield amounting to a thick almost complete coverage of large inorganic material in samples P10 and P11. Sample P4 was well covered with crystals of various sizes. Some large deposits had directional crystal growth in a columnar manner (Fig. 6(b)). This type of crystal growth could be observed in most samples although often to a lesser degree. EDX analysis of such areas yielded Ca/P ratios of 0.9 and (Ca + Mg)/P ratios of 1.1 (Fig. 7(a)). Sample P5 displayed large amounts of secondary growth (Fig. 6(c)) with a Ca/P ratio of 1.4 and (Ca + Mg)/P ratios of 1.5 (Fig. 7(b)). This type of secondary growth was also found on samples P5–P11. The surface coverage was non-homogeneous. Figs. 6(d) and (e) show two different areas of sample P8. One area (Fig. 6(d)) has a very high coverage of a $\sim 10\,\mu m$ thick calcium phosphate material. The large multi-directional cracks are probably due to specimen preparation although internal stresses may be responsible for the more regular crack patterns. In another area (Fig. 6(e)) the membrane is only thinly covered with inorganic material (around 2 μm thick). This difference in crystal coverage can (as above) be correlated with the patchy and uneven grafting of MAEP on the PTFE membranes [22].

When the thick deposits were analysed by EDX, a significant fraction (74–82%) of the total weight was not accounted for by the principal elements Ca, P and Mg. This fraction is higher than expected for oxygen contents in calcium phosphate minerals for which it is about 39–56%. For material thinner than the X-ray generation range in apatite (about 2 μm for P K-radiation), the totals would be reduced because some substrate would be included in the analysis. However, the totals were low for material much thicker than this, indicating that a significant fraction of the total weight could not be accounted for by Ca and P being present as a simple calcium phosphate phase. The difference is presumably made up by carbon and oxygen (in combination with hydrogen) which are not detected by the Be-window EDX detector on the SEM, and suggests that carbonates, hydroxides and additional bound water may be present. Some of the material was also analyzed in the TEM (see above), which was equipped with an X-ray detector capable of detecting the light elements, and the presence of at least some carbonate (mainly calcium carbonate) was confirmed.

Most commonly, precipitated calcium phosphate phases are studied using FTIR spectroscopy and XRD. However, in our MAEP-grafted PTFE samples these techniques did not enable us to identify the calcium phosphate phase due to overlaying bands in the FTIR spectra and a lack of crystallinity of the major inorganic phase. Instead, we investigated the calcium phosphate phases using EDX in SEM. This technique has been used previously to follow the Ca/P atomic ratios with soaking time in 1.5 × SBF for $Ca(OH)_2$ treated phosphorylated chitin fibers [32]. The Ca/P ratio of the actual coatings deposited on individual fibers was determined from individual coatings at high magnification (which is also the technique we used). Using this technique they found that the Ca/P ratio increased with time from 1.29 to 1.55. This was interpreted as the formation of an initial octacalcium phosphate (OCP) phase that rapidly transformed into a calcium-deficient apatite [32]. The result is comparable to our findings where the initial growth on MAEP-modified membranes in SBF has a (Ca + Mg)/P ratio of 1.1 and the secondary growth a (Ca + Mg)/P ratio of 1.5. Thus, the initial calcium phosphate phase is non-apatitic, presumably Brushite ($CaHPO_4 \cdot 2H_2O$) or Monetite ($CaHPO_4$) mixed with small amounts of the magnesium analogue. The subsequent growth is approaching an apatitic mineral phase, possibly calcium-deficient apatite or tricalcium phosphate ($Ca_3(PO_4)_2$).

4. Conclusion

The surface modifications (i.e. AAc and MAEP grafting) of PTFE membranes investigated in this study led to an increase in hydrophilicity of the surface. This is in turn a key factor in altering the surface properties of a material from being one that is unaffected in SBF to one which successfully induces nucleation in this *in vitro* test media. It appears that the nature of the inorganic materials formed is also dependant on the structure of the grafted monomer (i.e. MAEP or AAc). Results suggest that in addition to an apatite-like material (or tricalcium phosphate) on the MAEP-grafted samples, Brushite or Monetite is also forming. The inorganic material on the AAc-grafted sample is difficult to identify because of the presence of the calcium ions associated with the carboxylate groups from the pAAc units. Although

the AAc-grafted sample A3 induced calcium phosphate growth this modification is not expected to be ideal from a biomaterials perspective since the surface of the PTFE membrane was drastically altered resulting in partial blocking of the pores in the membrane. In contrast, the MAEP-modified samples with an external surface coverage of 44% or above are promising as improved biomaterials since the surface is altered only at a molecular level and yet the modified materials are able to induce calcium phosphate nucleation.

Acknowledgments

As always we are most appreciative for help from Dr. Llew Rintoul (CIDC, QUT) with FTIR spectroscopy. Dr. Robert A. Johnson (QUT) is greatly acknowledged for supplying the PTFE membrane. Dr L. Grøndahl acknowledges a QUT postdoctoral fellowship.

References

1. Y. IKADA, *Biomaterials* **15** (1994) 725.
2. B. KASEMO and J. LAUSMAA, *Environ. Health Perspect.* **102** (1994) 41.
3. O. N. TRETINNIKOV, K. KATO and Y. IKADA, *J. Biomed. Mater. Res.* **28** (1994) 1365.
4. S. KAMEI, N. TOMITA, S. TAMAI, K. KATO and Y. IKADA, *ibid.* **37** (1997) 384.
5. E. DALAS, J. K. KALLITSIS and P. G. KOUTSOUKOS, *Langmuir* **7** (1991) 1822.
6. K. JAMES, H. LEVENE, J. R. PARSONS and J. KOHN, *Biomaterials* **20** (1999) 2203.
7. S. H. LI, Q. LUI, J. R. de WIJN, B. L. ZHOU and K. de GROOT, *ibid.* **18** (1997) 389.
8. M. TANAHASHI and T. MATSUDA, *J. Biomed. Mater. Res.* **34** (1997) 305.
9. T. KOKUBO, H. KUSHITANI, S. SAKKA, T. KITSUGI and T. YAMAMURO, *ibid.* **24** (1990) 721.
10. Y. TAMADA, T. FURUZONO, T. TAGUCHI, A. KISHIDA and M. AKASHI, *J. Biomater. Sci. Polymer Edn.* **10** (1999) 787.
11. M. R. MUCALO, Y. YOKOGAWA, T. SUZUKI, Y. KAWAMOTO, F. NAGATA and K. NISHIZAWA, *J. Mater. Sci. Mater. Med.* **6** (1995) 658.
12. M. R. MUCALO, Y. YOKOGAWA, M. TORIYAMA, T. SUZUKI, Y. KAWAMOTO, F. NAGATA and K. NISHIZAWA, *ibid.* **6** (1995) 597.
13. H. M. KIM, F. MIYAJI, T. KOKUBO and T. NAKAMURA, *ibid.* **8** (1997) 341.
14. P. LI, C. OHTSUKI, T. KOKUBO, K. NAKANISHI, N. SOGA, T. NAKAMURA and T. YAMAMURO, *ibid.* **4** (1993) 127.
15. M. M. PEREIRA, A. E. CLARK and L. L. HENCH, *J. Am. Ceram. Soc.* **78** (1995) 2463.
16. A. L. OLIVEIRA, C. ELVIRA, R. L. REIS, B. VAZQUEZ and J. SAN ROMAN, *J. Mater. Sci. Mater. Med.* **10** (1999) 827.
17. R. L. REIS, A. M. CUNHA, M. H. FERNANDES and R. N. CORREIA, *ibid.* **8** (1997) 897.
18. M. HAMADOUCHE, A. MEUNIER, D. C. GREENSPAN, C. BLANCHAT, J. P. ZHONG, G. P. LA TORRE and L. SEDEL, *J. Biomed. Mater. Res.* **52** (2000) 422.
19. C. S. MAAS, D. R. GNEPP and J. BUMPOUS, *Arch. Otolaryngol. Head Neck Surg.* **119** (1993) 1008.
20. A. PIATTELLI, A. SCARANO and M. PAOLANTONIO, *Biomaterials* **17** (1996) 1725.
21. A. M. BARBE, J. P. BARTLEY, A. L. JACOBS and R. A. JOHNSON, *J. Mem. Sci.* **145** (1998) 67.
22. L. GRØNDAHL, F. CARDONA, K. CHIEM and E. WENTRUP-BYRNE, *J. Appl. Polym. Sci.* **86** (2002) 2550.
23. A. C. TAS, *Biomaterials* **21** (2000) 1429.
24. G. BEAMSON and D. BRIGGS, in ''The Scienta ESCA300 Database'' (Wiley, New York, 1992).
25. C. Y. LIANG and S. KRIMM, *J. Chem. Phys.* **25** (1956) 563.
26. I. ISHIGAKI, N. KAMIYA, T. SUGO and S. MACHI, *Polym. J.* **10** (1978) 513.
27. S. TURMANOVA, A. TRIFONOV, O. KALAIJIEV and G. KOSTOV, *J. Memb. Sci.* **127** (1997) 1.
28. B. O. FOWLER, E. C. MORENO and W. E. BROWN, *Arc. Oral. Biol.* **11** (1966) 477.
29. M. R. MUCALO, M. TORIYAMA, Y. YOKOGAWA, T. SUZUKI, Y. KAWAMOTO, F. NAGATA and K. NISHIZAWA, *J. Mater. Sci. Mater. Med.* **6** (1995) 409.
30. C. H. PARK, S. Y. NAM, Y. M. LEE and W. KUJAZSKI, *J. Mem. Sci.* **164** (2000) 121.
31. M. RÄTZSCH, H. BUCKA, S. S. IVANCHEV, A. M. MESH and KHAIKINE, *J. Appl. Polym. Sci.* **77** (2000) 711.
32. Y. YOKOGAWA, J. PAZ REYES, M. R. MUCALO, M. TORIYAMA, Y. KAWAMOTO, T. SUZUKI, K. NISHIZAWA, F. NAGATA and T. KAMAYAMA, *J. Mater. Sci. Mater. Med.* **8** (1997) 407.

Received 25 March
and accepted 20 August 2002